

Universal quantum computing with nanowire double quantum dots

P. Xue

Department of Physics, Southeast University, Nanjing 211189, P. R. China

(Dated: December 4, 2018)

We show a method for implementing universal quantum computing using a singlet and triplets of nanowire double quantum dots coupled to a one-dimensional transmission line resonator. This method is attractive for both quantum computing and quantum control with inhibition of spontaneous emission, enhanced spin qubit lifetime, strong coupling and quantum nondemolition measurements of spin qubits. We analyze the performance and stability of all required operations and emphasize that all techniques are feasible with current experimental technology.

PACS numbers: 03.67.Mn, 42.50.Pq, 73.21.La, 03.67.Lx

I. INTRODUCTION

A quantum computer comprising many two-level systems—qubits, exhibits coherent superpositions and entanglement. Quantum computing, which is based on these features, enables some computational problems to be solved faster than would ever be possible with a classical computer [1], and exponentially speeds up solutions to other problems over the best known classical algorithms [2], is currently attracting enormous interests. Among the promising candidates for quantum computing, solid-state implementations such as spin qubits in quantum dots [3] and bulk silicon [4], and charge qubits in bulk silicon [5] and in superconducting Josephson junctions [6], are especially attractive because of stability and expected scalability of solid-state systems; of these competing technologies, semiconductor double quantum dots (DQDs) are particularly important because of the combination spin and charge manipulations to take advantage of long memory times associated with spin states and at the same time to enable efficient readout and coherent manipulation of charge states.

Our goal is to develop a realizable architecture for semiconductor quantum computation. The qubit is manifested as a nanowire (NW) quantum dot pair such that each having an electron and thus the singlet and one of the triplets of two-electron states correspond to the logical state $|0\rangle$ and the orthogonal state $|1\rangle$. The resonator-assisted interaction between DQDs and a microwave transmission line resonator (TLR) is used to implement a universal set of quantum gates and readout of the qubits.

From two points, we show the advantages of our scheme compared to the previous proposals on semiconductor quantum computation. Firstly, for the previous proposals which make use of single or double quantum dots defined by a two-dimensional electron gas (2DEG) [7–14], it would be difficult to implement a double-dot in a planar resonator with lateral dots, shaped in a 2DEG by surface gates. The reason being is that it would be difficult to prevent absorption of microwaves in the 2DEG unless one can make the electric field non-zero only in the double-dot region, which is not realistic experimentally yet. Our strategy is to use the two-electron states of DQDs inside NWs instead of 2DEG, which is

more realistic for implementing quantum computing experimentally.

Secondly, there are previous proposals making use of NW DQDs [15], in which the spin-orbit interaction is used to couple the spins and resonator. However the weak coupling between the DQD spins and resonator mode is a challenge in experiments. Our strategy to enhance the interaction is to make use of the coupling between the electric dipole of charge states of DQDs and resonator, which is much stronger compared to that in [15]. However the decoherence of charge states is another obstacle. In this work, combining the advantages of spin and charge states and avoiding the weak points of both, we propose a different mechanism, namely via resonator-assisted interaction which leads to a strong coupling between the resonator photons and effective electric dipole of the state $|0\rangle$ and an ancillary state of DQDs, while the state $|1\rangle$ is driven by a classical field, and then eventually implements quantum control on the singlet and one of the triplet spin states. Thus we encode the quantum information in spin states and the quantum control is implemented via the charge dipole transition which is driven by a TLR.

A solid-state realization cavity QED is proposed in Sec. II and then we discuss the case where the resonator and qubit are tuned on- and off-resonance which can be used to implement a universal set of gates including single- and two-qubit gates in Sec. III A-C. The initialization of qubit states can be implemented by an adiabatic passage shown in Sec. III D. The readout of qubits can be realized via microwave irradiation of the TLR by probing the transmitted or reflected photons shown in Sec. III E. In Sec. III F, the main decoherence processes are dissipation of the TLR, charge-based relaxation and dephasing of the NW DQDs occurring during gate operations and transportation of qubits, and spin dephasing limited by hyperfine interactions with nuclei. By numerical analysis we show all gate operations and measurements can be implemented within the coherent life time of qubits. Thus we address all Divincenzo criteria [16] and show all play important roles in the dynamics of the two-electron system but none represents a fundamental limit for quantum computing. We make a summary in Sec. IV.

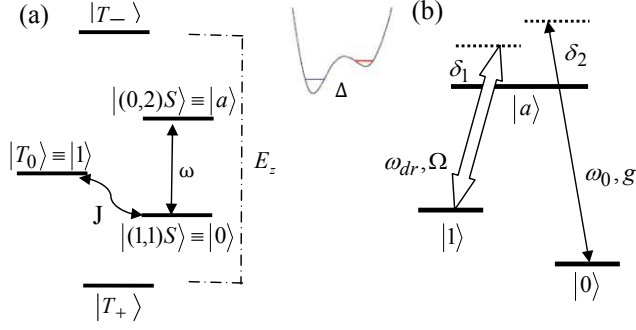


FIG. 1: (a) Energy level diagram showing the $(0, 2)$ and $(1, 1)$ singlets, the three $(1, 1)$ triplets and qubit states $|(1, 1)S\rangle$ and $|T_0\rangle$ with the energy gap J (the exchange energy $\sim T/10$). Schematic of the double-well potential with an energy offset Δ provided by the external electric field. (b) The relevant three-level structure of DQDs. The dipole transition $|0\rangle \rightarrow |a\rangle$ is coupled to the fundamental mode of the resonator with the coupling coefficient g and detuning δ_2 , while the transition $|1\rangle \rightarrow |a\rangle$ is driven by a classical field with the Rabi frequency Ω and detuning δ_1 .

II. SYSTEM: SOLID-STATE REALIZATION OF CAVITY QED

A. The Hamiltonian

We consider the system with two electrons located in adjacent quantum dots coupling via tunneling. Imagine one of the dots is capacitively coupled to a TLR [11–14]. We assume that the left dot (L) is red-shifted with respect to the right dot (R) and that the lowest conduction level of the left dot is detuned by Δ with respect to the right one.

In the $(1, 1)$ regime, with an external magnetic field $B_z = 1\text{T}$ along z axis the ground state manifold is given by the spin aligned states

$$|T_+\rangle = \hat{e}_{L\uparrow}^\dagger \hat{e}_{R\uparrow}^\dagger |vac\rangle = |\uparrow\uparrow\rangle$$

and

$$|T_-\rangle = \hat{e}_{L\downarrow}^\dagger \hat{e}_{R\downarrow}^\dagger |vac\rangle = |\downarrow\downarrow\rangle,$$

and the spin-anti-aligned states

$$|T_0\rangle = \frac{1}{\sqrt{2}}(\hat{e}_{L\uparrow}^\dagger \hat{e}_{R\downarrow}^\dagger + \hat{e}_{L\downarrow}^\dagger \hat{e}_{R\uparrow}^\dagger) |vac\rangle = \frac{1}{\sqrt{2}}(|\downarrow\uparrow\rangle + |\uparrow\downarrow\rangle)$$

and

$$|(1, 1)S\rangle = \frac{1}{\sqrt{2}}(\hat{e}_{L\uparrow}^\dagger \hat{e}_{R\downarrow}^\dagger - \hat{e}_{L\downarrow}^\dagger \hat{e}_{R\uparrow}^\dagger) |vac\rangle = \frac{1}{\sqrt{2}}(|\downarrow\uparrow\rangle - |\uparrow\downarrow\rangle)$$

with energy gaps due to the Zeeman splitting and exchange energy shown in Fig. 1. The notation (n_L, n_R) labels the number of electrons in the left and right quantum dots. The doubly occupied state $|(0, 2)S\rangle$ is coupled

via tunneling T to the singlet state $|(1, 1)S\rangle$. The double-dot system can be described by an extended Hubbard Hamiltonian

$$\begin{aligned} \hat{H} = & (E_{os} + \mu) \sum_{i,\sigma} \hat{n}_{i,\sigma} - T \sum_{\sigma} (\hat{c}_{L,\sigma}^\dagger \hat{c}_{R,\sigma} + \text{hc}) \\ & + U \sum_i \hat{n}_{i,\uparrow} \hat{n}_{i,\downarrow} + W \sum_{\sigma,\sigma'} \hat{n}_{L,\sigma} \hat{n}_{R,\sigma'} + \Delta \sum_{\sigma} (\hat{n}_{L,\sigma} - \hat{n}_{R,\sigma}) \end{aligned} \quad (1)$$

for $\hat{c}_{i,\sigma}$ ($\hat{c}_{i,\sigma}^\dagger$) annihilating (creating) an electron in quantum dot $i \in \{L, R\}$ with spin $\sigma \in \{\uparrow, \downarrow\}$, $\hat{n}_{i,\sigma} = \hat{c}_{i,\sigma}^\dagger \hat{c}_{i,\sigma}$ a number operator, and Δ an energy offset yielded by the external electric field along x axis shown in Fig. 2. The first term corresponds to on-site energy E_{os} plus site-dependent field-induced corrections μ . The second term accounts for $i \leftrightarrow j$ electron tunneling with rate T , the third term is the on-site charging cost U to put two electrons with opposite spin in the same dot, and the fourth term corresponds to inter-site Coulomb repulsion, and the forth term is the cost of putting one electron at site i and another electron at site j .

In the basis $\{|(1, 1)S\rangle, |(0, 2)S\rangle\}$, the Hamiltonian can be deduced as

$$\hat{H}_d = -\Delta |(0, 2)S\rangle \langle(0, 2)S| + T |(1, 1)S\rangle \langle(0, 2)S| + \text{hc}. \quad (2)$$

With the energy offset Δ , degenerate perturbation theory in the tunneling T reveals an avoided crossing at this balanced point between $|(1, 1)S\rangle$ and $|(0, 2)S\rangle$ with an energy gap $\omega = \sqrt{\Delta^2 + 4T^2}$, and the effective tunneling between the left and right dots with the biased energies Δ is changed from T to $\omega/2$.

We choose the singlet state and one of the triplet states as our qubit:

$$|0\rangle \equiv |(1, 1)S\rangle, \quad |1\rangle \equiv |T_0\rangle, \quad (3)$$

and the doubly occupied state as an ancillary state

$$|a\rangle \equiv |(0, 2)S\rangle. \quad (4)$$

The essential idea is to use an effective electric dipole moment associated with singlet states $|0\rangle$ and $|a\rangle$ of a NW DQD coupled to the oscillating voltage associated with a TLR shown in Fig. 2. We consider a TLR with length L , the capacitance per unit length C_0 and the characteristic impedance Z_0 . A capacitive coupling C_c between the NW DQD and TLR causes the electron charge state to interact with excitations in the transmission line. We assume that the dot is much smaller than the wavelength of the resonator excitation, so the interaction strength can be derived from the electrostatic potential energy of the system

$$\hat{H}_{\text{int}} = e\hat{V}v|a\rangle \langle a|, \quad (5)$$

where e is the electron charge,

$$v = \frac{C_c}{C_{\text{tot}}}, \quad \hat{V} = \sum_n \sqrt{\frac{\hbar\omega_n}{LC_0}} (\hat{a}_n + \hat{a}_n^\dagger) \quad (6)$$

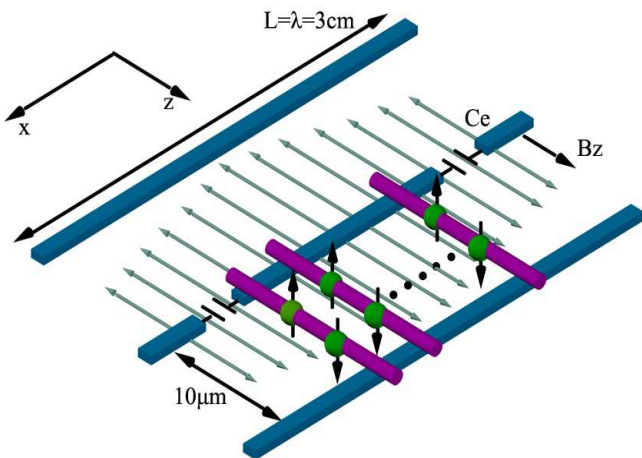


FIG. 2: Schematic of NW DQDs capacitively coupled to the TLR. The coupling can be switched on and off via the external electric field. The DQD confinement can be achieved by barrier materials or by external gates (not shown).

is the voltage on the TLR near the left dots, $\hat{a}_n, \hat{a}_n^\dagger$ are the creation and annihilation operators for the mode $k_n = [(n+1)\pi]/L$ of the TLR, and C_{tot} is the total capacitance of the DQD. The fundamental mode frequency of the TLR is $\omega_0 = \pi/LZ_0C_0$. The TLR is coupled to a capacitor C_e for writing and reading the signals. Neglecting the higher modes of the TLR and working in the rotating frame with the rotating wave approximation, we obtain an effective Hamiltonian as

$$\hat{H}_{\text{eff}} = \omega_0 \hat{a}^\dagger \hat{a} + \omega |a\rangle \langle a| + g(\hat{a}|a\rangle \langle 0| + \text{hc}) \quad (7)$$

with \hat{a} (\hat{a}^\dagger) the annihilation (creation) operator of the resonator field, and the effective coupling coefficient

$$g = \frac{1}{2} e \frac{C_c}{LC_{\text{tot}}C_0} \sqrt{\frac{\pi}{Z_0}} \sin 2\theta \quad (8)$$

with $\theta = \frac{1}{2} \tan^{-1}(\frac{2T}{\Delta})$.

The interaction between the TLR and qubit states is switchable via tuning the electric field along x axis. In the case of the energy offset yielded by the electric field $\Delta \approx 0$, we obtain the maximum value of the coupling between the TLR and singlets in DQDs. That is so-called the optimal point. Whereas $\Delta \gg T$, θ tends to 0, the interaction is switched off.

The transition from $|1\rangle$ to $|a\rangle$ is driven by a classical laser field with a Rabi frequency Ω . The interaction Hamiltonian is given by

$$\hat{H}_{\text{dr}} = \Omega e^{-i\omega_{\text{dr}}t} |a\rangle \langle 1| + \Omega e^{i\omega_{\text{dr}}t} |1\rangle \langle a|, \quad (9)$$

where ω_{dr} is the drive frequency.

B. Physical realization

A realization of DQDs defined using local gates to electrostatically deplete InAs NWs grown by chemical beam

epitaxy was reported [17]. The quantum-mechanical tunneling T between the two quantum dots is about $0 - 150 \mu\text{eV}$ [17]. Thus at the optimal point $\Delta \approx 0$ where the coupling is strongest, the energy gap between the singlets is about $\omega \sim 2T \simeq 0 - 72 \text{GHz}$. A small-diameter ($\sim 65 \text{nm}$), long-length ($\sim 270 \text{nm}$) and $g^* = -13$ [18] InAs NW is positioned perpendicularly to the transmission line and containing DQDs that are elongated along the NW shown in Fig. 2. The external magnetic field along z axis is about $B_z = 1 \text{T}$ to make sure that the energy splitting $E_z = g^* \mu_B B_z$ between the two triplet states $|T_\pm\rangle$ is larger than ω .

The TLR can be fabricated with existing lithography techniques [19]. The dots can be placed within the TLR formed by the transmission line to strongly suppress the spontaneous emission. To prevent a current flow, the NW and transmission line need to be separated by some insulating coating material obtained for example by atomic layer deposition. We assume that the TLR is 3cm long and $10 \mu\text{m}$ wide, $Z_0 = 50 \Omega$ which implies for the fundamental mode $\omega_0 = \pi/LC_0Z_0 = 2\pi \times 10 \text{GHz}$. In practice, careful fabrication permits a strong coupling capacitance, with $C_{\text{tot}} \approx 5.1C_c$ [17], so that the coupling coefficient $g \sim 2\pi \times 120 \text{MHz}$ is achievable due to the numerical estimations in Eq. (8). The frequency ω_0 and coupling coefficient g can be tuned via LC_0 . With a magnetic field about 1T the resonators in coplanar waveguides with $Q \sim 10^3 - 10^4$ have already been demonstrated in [20].

The effect of photon assisted tunneling (PAT) in our system is harmful because it destroys the qubit by lifting spin-blockade. To avoid this, our strategy is to close enough the tunneling barriers to the leads.

III. UNIVERSAL QUANTUM COMPUTING

A. Single-qubit gate operations

First we consider the zero-detuning case in which the fundamental mode frequency of the TLR is $\omega_0 \approx \omega$. The Hamiltonian (7) has the same form as the Jaynes-Cummings Hamiltonian of a two-level system with a single-mode resonator field. In the case when the TLR is initially in the photon number state $|n\rangle_r$, the time evolution of the system, governed by the Hamiltonian (7), is described by

$$|0\rangle |n\rangle_r \rightarrow \cos \sqrt{n}gt |0\rangle |n\rangle_r - i \sin \sqrt{n}gt |a\rangle |n-1\rangle_r, \quad (10)$$

$$|a\rangle |n\rangle_r \rightarrow -i \sin \sqrt{n+1}gt |0\rangle |n+1\rangle_r + \cos \sqrt{n+1}gt |a\rangle |n\rangle_r.$$

From the Hamiltonian of a drive on the DQDs shown in (9), it is straightforward to see that a pulse of duration t results in the following rotation:

$$\begin{aligned} |1\rangle &\rightarrow \cos \frac{\Omega}{2}t |1\rangle - \sin \frac{\Omega}{2}t |a\rangle, \\ |a\rangle &\rightarrow -i \sin \frac{\Omega}{2}t |1\rangle + \cos \frac{\Omega}{2}t |a\rangle. \end{aligned} \quad (11)$$

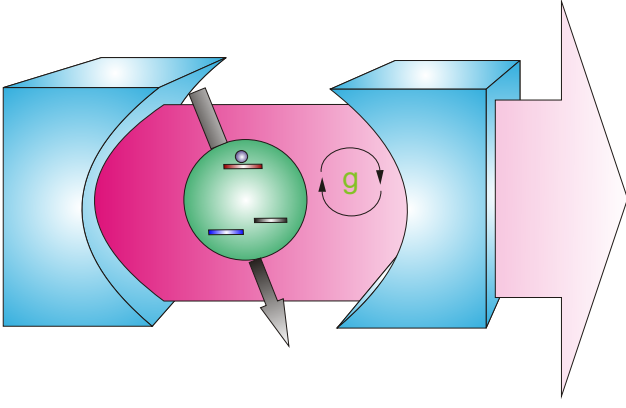


FIG. 3: Standard representation of a cavity QED system, comprising a single mode of the electromagnetic field in a cavity coupled with a strength g to a three-level system and a classical drive.

It has been reported in [21] that the structure of the TLR and qubits tuned on-resonance can be used to implement an entangling gate on spin qubits of NW DQDs via the adiabatic evolution of the dark states.

In this paper, we show a different proposal and consider the case where the TLR and qubits are tuned off resonant, which leads to lifetime enhancement of the qubits and implements coherent control. Assume that the classical field and TLR are detuned from the transitions by $\delta_1 = \omega_{\text{dr}} - (\omega - J)$ and $\delta_2 = \omega_0 - \omega$, respectively, the Hamiltonian for single DQD coupled to the TLR and driven by a classical field is

$$\hat{H}_{1\text{q}} = \omega_0 \hat{a}^\dagger \hat{a} + \omega |a\rangle \langle a| + g(\hat{a} |a\rangle \langle 0| + \Omega e^{-i\omega_{\text{dr}} t} |a\rangle \langle 1| + \text{hc}) \quad (12)$$

If $\delta_1, \delta_2 \gg \Omega, g$ is satisfied, the upper level $|a\rangle$ can be adiabatically eliminated. We then obtain the effective Hamiltonian of the system as

$$\hat{H}_{1\text{q}}^{\text{eff}} = \frac{\Omega^2}{\delta_1} |1\rangle \langle 1| + \frac{g^2}{\delta_2} \hat{a}^\dagger \hat{a} |0\rangle \langle 0| + \lambda(\hat{a} |1\rangle \langle 0| + \text{hc}), \quad (13)$$

where $\lambda = \Omega g / 2(\delta_1 + \delta_2)$. The first two terms describe the Stark shifts for the spin states $|0\rangle$ and $|1\rangle$, induced by the classical field and resonator mode, respectively. The last term is the Raman coupling of the two spin states.

For single spin qubits in $\{|0\rangle, |1\rangle\}$ coupled with effective strength λ to the TLR, driven by a classical field which is detuned from the TLR, the Hamiltonian (13) can be used to implement single qubit rotations along x axis via the Rabi oscillation between the states $|0\rangle$ and $|1\rangle$ shown in Fig. 3.

B. Two-qubit gate operations

Now we consider there are two spin qubits coupled to the TLR. From the Hamiltonian (13), in the case of $\delta_2 - \delta_1 \gg \lambda$, there is no energy exchange between the

DQD system and TLR. The energy conserving transitions are between $|1_1 0_2\rangle |n\rangle_{\text{r}}$ and $|0_1 1_2\rangle |n\rangle_{\text{r}}$. The effective Rabi frequency for the transitions between these states, mediated by $|0_1 0_2\rangle |n+1\rangle_{\text{r}}$ and $|1_1 1_2\rangle |n-1\rangle_{\text{r}}$ is given by

$$\begin{aligned} \lambda' &= \frac{\langle 1_1 0_2 n | \hat{H}_{\text{tot}} | 0_1 0_2 n + 1 \rangle \langle 1_1 0_2 n + 1 | \hat{H}_{\text{tot}} | 0_1 1_2 n \rangle}{\delta_2 - \delta_1} \\ &+ \frac{\langle 1_1 0_2 n | \hat{H}_{\text{tot}} | 1_1 1_2 n - 1 \rangle \langle 1_1 1_2 n - 1 | \hat{H}_{\text{tot}} | 0_1 1_2 n \rangle}{-(\delta_2 - \delta_1)} \\ &= \frac{\lambda^2}{\delta_2 - \delta_1}, \end{aligned} \quad (14)$$

where $\hat{H}_{\text{tot}} = \sum_{j=1,2} \hat{H}_{1\text{q}}^j$. The effective Hamiltonian for two qubits turns to be

$$\begin{aligned} \hat{H}_{2\text{q}} &= \sum_{j=i,2} \frac{g^2}{\delta_2} \hat{a}^\dagger \hat{a} |0\rangle_j \langle 0| + \frac{\Omega^2}{\delta_1} |1\rangle_j \langle 1| + \lambda' \hat{a} \hat{a}^\dagger (|1\rangle_j \langle 1| \\ &- |0\rangle_j \langle 0|) + \lambda' (|1\rangle_j \langle 0| \otimes |0\rangle_j \langle 1| + \text{hc}). \end{aligned} \quad (15)$$

The third and fourth terms are the photon-number dependent Stark shifts induced by the Raman transition, and the last term is the induced dipole coupling between the two spin qubits. If the resonator mode is initially in the vacuum state it will remain in the vacuum state throughout the process. Then the effective Hamiltonian for the two qubits is reduced to

$$\hat{H}_{2\text{q}}^{\text{eff}} = \sum_{j=1,2} \frac{\Omega^2}{\delta_1} |1\rangle_j \langle 1| + \lambda' (\hat{\sigma}_+^1 \hat{\sigma}_-^2 + \text{hc}), \quad (16)$$

where $\hat{\sigma}_+ = |1\rangle \langle 0|$ and $\hat{\sigma}_- = |0\rangle \langle 1|$.

The evolution of the effective two-qubit Hamiltonian can be used to implement an entangling two-qubit gate— \sqrt{i} SWAP. In a frame rotating at the qubit's frequency, the Hamiltonian (16) generates the evolution

$$\begin{aligned} U_{2\text{q}}(t) &= \prod_{j=1,2} \exp \left[-i \frac{\Omega^2}{\delta_1} t |1\rangle_j \langle 1| \right] \\ &\times \begin{pmatrix} 1 & 0 & 0 & 0 \\ 0 & \cos \lambda' t & i \sin \lambda' t & 0 \\ 0 & i \sin \lambda' t & \cos \lambda' t & 0 \\ 0 & 0 & 0 & 1 \end{pmatrix} \end{aligned} \quad (17)$$

Up to the phase factor, it corresponds at $t_{2\text{q}} = \pi / 4\lambda'$ to a \sqrt{i} SWAP logical operation. Up to single-qubit gates, the above operation is equivalent to the controlled-not gate. Together with single-qubit gates, the interaction $\hat{H}_{2\text{q}}^{\text{eff}}$ is therefore sufficient for universal quantum computing.

When the qubits are detuned from each other, the off-diagonal coupling provided by $\hat{H}_{2\text{q}}^{\text{eff}}$ is only weakly effective and the coupling is for all practical purposes turned off. Two-qubit logical gates in this setup can therefore be controlled by individually tuning the qubits. Moreover, single- and two-qubit logical operations on different qubits and pairs of qubits can both be realized simultaneously, a requirement of reach presently known thresholds for fault-tolerant quantum computation [22].

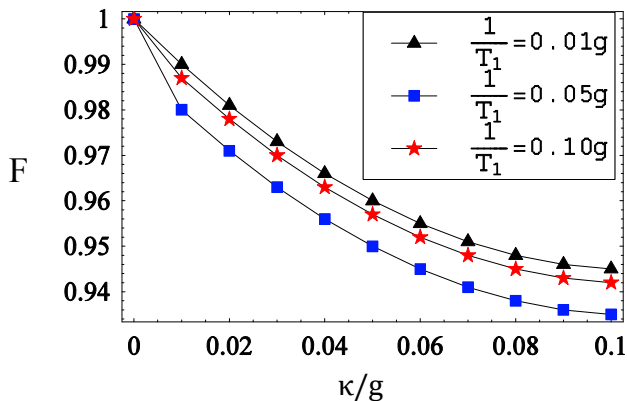


FIG. 4: (color online). Fidelity (F) of the two-qubit $\sqrt{i\text{SWAP}}$ gate vs the resonator decay rate κ with the experimental parameters $\{\omega_0, \omega, \omega_{\text{dr}}, g, \Omega\}/2\pi = \{10, 5, 9.74, 0.12, 1\}$ GHz. The triangled, stared, boxed lines describe the cases of the spontaneous emission rate of the singlet states $1/T_1 = 0.01g, 0.05g, 0.1g$, respectively.

Hence we have built a universal set of gates for quantum computing with semiconductor DQDs coupled to a resonator field. The feasibility of single-qubit gates has already been proved in [6] experimentally. For the two-qubit gate, we realize it with the off-resonant interaction between both qubits and TLR. With the experimental parameters $\{T, J, \omega_0, \omega, \omega_{\text{dr}}, g, \Omega\}/2\pi = \{2.5, 0.25, 10, 5, 9.74, 0.12, 1\}$ GHz, the detunings $\delta_1/2\pi = 4.99$ GHz and $\delta_2/2\pi = 5$ GHz, and the efficient coupling coefficients $\lambda = 3$ MHz and $\lambda' = 0.9$ MHz, we can estimate the time scaling for quantum computing. The operating time for the single-qubit rotation along x axis is $t_x \sim 1/\lambda \approx 300$ ns with the above parameters. The single-qubit rotation along z axis takes the same time scaling as the two-qubit gate in (16) t_{2q} which satisfies $\lambda' t_{2q} = \pi/4$ and is calculated as $t_{2q} \approx 1\mu\text{s}$.

C. Fidelity of two-qubit gates

Now we analyze the effect on gate operations due to noise and derive the fidelity of two-qubit gates. We use the two-qubit gate Eq. (17) as an example. With the time dependent fluctuations $\delta\lambda'(t)$ of the effective coupling coefficient λ' , the evolution operator of the system becomes

$$U'_{2q} = U_{2q} \exp \left[-i \int_0^{t_{2q}} dt \delta\lambda'(t) (\hat{\sigma}_+^1 \hat{\sigma}_-^2 + \hat{\sigma}_-^1 \hat{\sigma}_+^2) \right], \quad (18)$$

where the unwanted phase $\phi = \int_0^{t_{2q}} dt \delta\lambda'(t)$. The distribution of the unwanted phase becomes Gaussian distribution because λ' is in Gaussian distribution. With the parameters above, we numerically calculate the variances of the unwanted phase $\text{Var}(\phi) \sim 2 \times 10^{-3}\pi$.

Furthermore, the decoherence such as dephasing reduces the fidelity of gate operations as well. We an-

alyze the dephasing rate due to the variations of the AC Stark shift $g^2/\delta_2 \hat{a}^\dagger \hat{a} \hat{\sigma}_z$ (where $\hat{\sigma}_z = |0\rangle\langle 0| - |1\rangle\langle 1|$) caused by quantum fluctuations of the number of photon \bar{n} within the resonator. To determine the dephasing rate, we assume that the resonator is driven at the bare resonator frequency ω_0 and the pull of the resonance is small compared to the linewidth κ . The relative phase accumulated between the two singlet states $|0\rangle$ and $|a\rangle$ is $\vartheta(t) = 2\frac{g^2}{\delta_2} \int_0^t dt' n(t')$, which yields a mean phase advance $\langle \vartheta \rangle = 2g^2 \bar{n} t / \delta_2$. Dephasing can be evaluated by the decay of the correlator $\langle \exp \left[i \int_0^t dt' \vartheta(t') \right] \rangle$. If the resonator is not driven the photon number correlator rather decays at a rate κ and the rate of transmission on-resonance is $\gamma_\vartheta = \bar{n}\kappa/2$. In the dispersive regime, the dephasing rate is reduced to $\gamma_\vartheta = 8\bar{n} \left(\frac{g^2}{\delta_2}\right)^2 \frac{1}{\kappa}$.

From the analysis, we show that even the decoherence and noise occur over the gate operation, we can still implement a universal set of gates with high fidelities. In Fig. 4, we show the fidelity $F = \text{int} \langle \varphi | U_{2q}^\dagger \rho U_{2q} | \varphi \rangle_{\text{int}}$ of the two-qubit gate $\sqrt{i\text{SWAP}}$ as a function of the resonator decay κ and spontaneous emission of the DQD singlet state $1/T_1$, where ρ is the reduced density matrix calculated by solving the master equation with decoherence and tracing out the resonator photon, and $|\varphi\rangle_{\text{int}}$ is the initial states of the spin states. With the experimental parameters $\{\omega_0, \omega, \omega_{\text{dr}}, g, \Omega, \kappa, 1/T_1\}/2\pi = \{10, 5, 9.74, 0.12, 1, 0.001, 0.001\}$ GHz, the fidelity is achieved as high as 0.991.

For single-qubit $\hat{\sigma}_x$ gate, the unwanted phase is $\int_0^t dt \delta\lambda(t)$. With the same method, we can calculate the variance of the phases.

D. Initialization and transportation

Initialization of qubit states can be implemented by an adiabatic passage between the two singlet states $|0\rangle$ and $|a\rangle$ [10]. Controllably changing Δ allows for adiabatic passage to past the charge transition, with $|a\rangle$ as the ground state if $\Delta \gg T$ achieved. First we turn on the external electric field along x axis and prepare the two electrons of NW DQDs in the state $|a\rangle$ by a large energy offset Δ . We change θ in Eq. (8) adiabatically to $\pi/4$ by tuning the electric field, and then initialize the qubits in the state $|0\rangle$.

The SWAP operation [12], where a qubit state is swapped with a photonic state of the TLR, can be used to implement transmission of qubits. If there is no photon in the TLR, with the evolution time π/λ , a qubit is mapped to the photonic state in the TLR

$$(\alpha |0\rangle + \beta |1\rangle) |0\rangle_{\text{r}} \longrightarrow |0\rangle (\alpha |0\rangle + \beta |1\rangle)_{\text{r}}. \quad (19)$$

Then we switch off the coupling between this qubit and TLR and switch on that between the desired qubit and TLR via the local electric fields along x axis. After the

same evolution time, the previous qubit state is transmitted to the desired qubit via the interaction with the TLR. The time for transmitting a qubit to a photonic qubit in the TLR is about $t_{\text{tr}} = \pi/\lambda \approx 900\text{ns}$ with the experimental parameters shown in Sec. III.

E. Readout

To perform a measurement of qubits, the classical field and TLR are tuned from the respective transitions modeled by Eq. (13). In the dispersive regime ($\delta_1, \delta_2 \gg \Omega, g$), the energy gap between the dressed states $|0\rangle_r$ and $|1\rangle_r$ is $\omega_0 - g^2/\delta_2$ for the qubit in the state $|0\rangle$, while the energy gap ω_0 for the state $|1\rangle$ remains unchanged. The operator being probed is $\hat{\sigma}_z$ and the qubit-measurement apparatus interaction Hamiltonian is $g^2/\delta_2 \hat{a}^\dagger \hat{a} \hat{\sigma}_z$, such that $[\hat{\sigma}_z, g^2/\delta_2 \hat{a}^\dagger \hat{a} \hat{\sigma}_z] = 0$. Depending on the qubit being in the states $|0\rangle$ or $|1\rangle$ the transmission spectrum presents a peak of width κ (the resonator decay rate) at $\omega_0 - g^2/\delta_2$ or ω_0 . This dispersive pull of the resonator frequency is $0 \sim g^2/\kappa\delta_2$, and the pull is power dependent and decreases in magnitude for photon numbers inside the TLR [23]. Via microwave irradiation of the TLR by probing the transmitted or reflected photons, the readout of qubits can be realized and completed on a time scaling $t_m = 1/\gamma_\vartheta$, where γ_ϑ is the dephasing rate due to quantum fluctuations of the number of photon \bar{n} within the TLR shown in Sec. III C. Compared to the dephasing rate of transmission on resonance $\gamma_\vartheta = \bar{n}\kappa/2$, in the dispersive regime the phase noise induced by the AC Stark shift $g^2/\delta_2 \hat{a}^\dagger \hat{a} \hat{\sigma}_z$ results in the dephasing rate $\gamma_\vartheta = 8\bar{n}(\frac{g}{\delta_2})^2 \frac{1}{\kappa}$ and an enhanced lifetime of spin qubits. This approach can serve as a high efficiency quantum nondemolition dispersive readout of the qubit states: $P_1 = |0\rangle\langle 0|$; $P_2 = |1\rangle\langle 1|$. Readout of qubits takes the time $t_m \approx 1.5\text{ns}$ in the case $\bar{n} = 100$ with the experimental parameters shown above.

F. Decoherence

In Sec. III C, we show the decoherence occurring over the two-qubit gate operation, now we analyze the dominant noise sources of the system existing during all precessings, which include the spin phase noise due to hyperfine coupling, the charge-based dephasing and relaxation occurring during gate operations and transportation, and the photon loss due to the resonator decay. The characteristic charge dephasing with a rate T_2^{-1} . The time-ensemble-averaged dephasing time T_2^* is limited by hyperfine interactions with nuclear spins. Coupling to a phonon bath causes relaxation of the charge system in a time T_1 . The decay of the TLR κ is considered as another dominant source of decoherence.

The hyperfine interactions with the gallium arsenide host nuclei causes nuclear spin-related dephasing T_2^* .

The hyperfine field can be treated as a static quantity, because the evolution of the random hyperfine field is several orders slower than the electron spin dephasing. In the operating point, the most important decoherence due to hyperfine field is the dephasing between the singlet state $|(1,1)S\rangle$ and one of the triplet state $|T_0\rangle$. By suppressing nuclear spin fluctuation, the dephasing time can be obtained by quasi-static approximation as $T_2^* = 1/g\mu_B \langle \Delta B_n^z \rangle_{\text{rms}}$, where ΔB_n^z is the nuclear hyperfine gradient field between two coupled dots and rms means a root-mean-square time-ensemble average. A measurement of the dephasing time $T_2^* \sim 4\text{ns}$ was demonstrated in [15] and we expect coherently driving the qubit well prolong the T_2^* time up to $1\mu\text{s}$ and with echo up to $10\mu\text{s}$ [8].

For the charge relaxation time T_1 , the decay is caused by coupling qubits to a phonon bath. With the spin-boson model, the perturbation theory gives an overall error rate from the relaxation and incoherent excitation, with which one can estimate the relaxation time $T_1 \sim 1\mu\text{s}$ [12] which is studied in great detail for the GaAs quantum dot in 2DEG and similar rate is expected for NW quantum dots.

The charge dephasing T_2 rises from variations of the energy offset $\Delta(t) = \Delta + \epsilon(t)$ with $\langle \epsilon(t)\epsilon(t') \rangle = \int d\omega S(\omega) e^{i\omega(t-t')}$, which is caused by the low frequency fluctuation of the electric field. The gate bias of the qubit drifts randomly when an electron tunnels between the metallic electrode. Due to the low frequency property, the effect of the $1/f$ noise on the qubit is dephasing rather than relaxation. At the zero derivative point, compared to a bare dephasing time $T_b = 1/\sqrt{\int d\omega S(\omega)}$, the charge dephasing is $T_2 \sim \omega T_b^2$ near the optimal point $\Delta = 0$. The bare dephasing time $T_b \sim 1\text{ns}$ was observed in [24]. Then the charge dephasing is estimated as $T_2 \sim 10 - 100\text{ns}$. Using quantum control techniques, such as better high- and low-frequency filtering of electronic noise, T_b exceeding $1\mu\text{s}$ was observed in 2DEG [8] (we assume a similar result for the present case), which suppresses the charge dephasing.

The quality factor Q of the TLR in the microwave domain can be achieved 10^6 [19]. In practice, the local external magnetic field 1T reduces the limit of the quality factor to $Q \sim 10^3 - 10^4$ [20]. The dissipation of the TLR $\kappa = \omega_0/Q$ leads to the decay time about $100\text{ns} - 1\mu\text{s}$ with the parameters $\omega_0 = 2\pi \times 10\text{GHz}$.

Thus, the operating times of all these gates $\{t_x, t_{2q}, t_{\text{tr}}, t_m\} = \{300\text{ns}, 1\mu\text{s}, 900\text{ns}, 1.5\text{ns}\}$ are less than the minimum decoherence time.

IV. SUMMARY

Advances in fabrication have led to the development of solid-state systems, with obvious potential for quantum computing. The Heisenberg exchange coupling, optical dipole-dipole interactions, capacitive coupling, and opti-

cal cavity-mediate interactions between spin and charge states can be used to realize controlled quantum state operations. In this paper we focus on NW DQDs quantum computer which would capitalize on chip fabrication technology and could be hybridized with existing computers. We propose a realization of cavity QED via electrically controlled semiconductor spins of NW DQDs coupled to a microwave TLR on a chip. Combining the advantages of spin and charge states and avoiding the weak points of both, we propose a mechanism to achieve a scalable architecture for quantum computing with NW DQDs inside a TLR, namely via resonator-assisted interaction which leads to an efficient, strong coupling between the resonator photon and effective electric dipole of DQDs. Thus we encode the quantum information in spin states and the gate operation is implemented via the charge dipole transition which is driven by a resonator. Initialization of qubits can be realized with an adiabatic passage. With the switchable coupling to the TLR, we can implement a universal set of quantum gates on any qubit. Because of the switchable coupling between the

double-dot pairs and TLR, we can apply this entangling gate on any two qubits without affecting others, which is not trivial for implementing scalable quantum computing and generating large entangled state. The fidelities of the gates in our protocol are studied including all kinds of major decoherence, with promising results for reasonably achievable experimental parameters and these results demonstrate the practicality by way of current experimental technologies. Our work shows how an experiment can be performed under existing conditions to demonstrate the first architecture for quantum computing for spin qubits in quantum dots in the laboratory.

Acknowledgments

This work has been supported by National Natural Science Foundation of China, Grant No. 11004029, Jiangsu Province Natural Science Foundation, Grant No. BK2010422, and Southeast University Startup fund.

-
- [1] L. Grover, Phys. Rev. Lett. **79**, 325 (1997).
 [2] P.W. Shor, Proc. 35th Annual Symp. on Found. of Comp. Sci. (Los Alamitos, CA: IEEE Computer Society Press, 1994) 124.
 [3] D. Loss, D.P. DiVincenzo, Phys. Rev. A **57**, 120 (1998).
 [4] B.E. Kane, Nature **393**, 133 (1998).
 [5] S.E.S. Andresen et al., Nanolett. **7**, 2000 (2007).
 [6] A. Wallraff et al., Phys. Rev. Lett. **95**, 060501 (2005).
 [7] A. Imamoglu et al., Phys. Rev. Lett. **83**, 4204 (1999).
 [8] J.R. Petta et al., Science **309**, 2180 (2005).
 [9] A.C. Johnson, Nature **435**, 925 (2005).
 [10] J.M. Taylor et al., Phys. Rev. B **76**, 035315 (2007).
 [11] G. Burkard, A. Imamoglu, Phys. Rev. B **74**, 041307(R) (2006).
 [12] J.M. Taylor, M.D. Lukin, arXiv: cond-mat/0605144.
 [13] Z.R. Lin et al., Phys. Rev. Lett. **101**, 230501 (2008).
 [14] P. Xue, Phys. Lett. A **374**, 2601 (2010).
 [15] M. Trif, V.N. Golovach and D. Loss, Phys. Rev. B **77**, 045434 (2008).
 [16] D.P. DiVincenzo, Fortschr. Phys. **48**, 771 (2000).
 [17] C. Fasth, A. Fuhrer, M.T. Björk and L. Samuelson, Nano Lett. **5**, 1487 (2005).
 [18] M.T. Björk et al., Phys. Rev. B **72**, 201307(R) (2005).
 [19] A. Wallraff et al., Nature **431**, 162 (2004).
 [20] L. Frunzio et al., Applied Superconductivity, IEEE Transactions on **15**, 860 (2005).
 [21] S.B. Zheng, Phys.Rev. Lett. **95**, 080502 (2005); P. Xue, Chin. Phys. Lett. **27**, 060301 (2010).
 [22] D. Aharonov and M. Ben-Or, in *Proceedings of the 37th Annual Symposium on Foundations of Computer Science* (IEEE Computer Society Press, Los Alamitos, CA, 1996), p. 46.
 [23] A. Blais et al., Phys. Rev. A **69**, 062320 (2004); J. Gambetta et al., Phys. Rev. A **74**, 042318 (2006); A. Blais et al., Phys. Rev. A **75**, 032329 (2007).
 [24] T. Hayashi et al., Phys. Rev. Lett. **91**, 226804 (2003); J.R. Petta et al., *ibid* **93**, 186802 (2004).